Photoluminescence properties of thin-film SiO$_x$C$_y$ deposited by O-Cat CVD technique using MMS and TEOS

Manmohan Jain
SEES, Electrical Engineering Department
CINVESTAV-IPN
Mexico City, Mexico
manmohan@cinvestav.mx

J. R. Ramos-Serrano
Program of Nanoscience and Nanotechnology
CINVESTAV-IPN
Mexico City, Mexico
juan.ramos@cinvestav.mx

Ateet Dutt
Instituto de Investigaciones en Materiales
Universidad Nacional Autónoma de México,
Mexico City, Mexico
adutt@iim.unam.mx

Yasuhiro Matsumoto
SEES, Electrical Engineering Department
CINVESTAV-IPN
Mexico City, Mexico
ymatsumo@cinvestav.mx

Abstract— **This work aims to evaluate the properties of deposited SiO$_x$C$_y$ thin films by means of organic catalytic chemical vapor deposition (O-Cat CVD) technique. The employed precursors were Monomethyl Silane (MMS; (CH$_3$-SiH$_3$)) and Tetra-ethyl orthosilicate [TEOS; (Si(OC$_2$H$_5$)$_4$)], which corresponded to gaseous and liquid sources, respectively. The deposition chamber worked under a reactant atmosphere of hydrogen (H$_2$) and oxygen (O$_2$), likewise the use of tantalum (T$_a$) as a catalyst for MMS precursor. TEOS was used at the Argon atmosphere and tungsten (W) as a catalyst. The deposition time was varied from 20 to 30 min in order to evaluate its influence on the luminescent properties of the deposited films. Chemical and bonding-state characterization were performed through Fourier transform infrared (FTIR) and X-ray Photoelectron Spectroscopy (XPS) techniques. The measurements of thickness and refractive index of the thin films were obtained by ellipsometry. Optical properties were evaluated by photoluminescence spectroscopy. The FTIR showed the peak shifting from the stoichiometric stretching value of Si-O-Si bonding (1080 cm^{-1}) to 1025 cm^{-1} and 1036 cm^{-1} for MMS and TEOS precursors, respectively. The Si-O-Si bonding shift might come due to the oxygen deficiency in the prepared samples. Through XPS measurements, it was possible to determine different bonding states and their amount through the formation of SiO$_x$C$_y$ thin films; however, the sample deposited with TEOS shows its nature closer to the SiO$_x$ phase in comparison to MMS deposited thin films. The thickness of thin films increased proportionately with the increment of deposition time. Moreover, the red-shifted PL spectrum was determined for the MMS deposited samples in comparison to TEOS deposited samples. Intense emission in a broad region of the visible spectrum was observed without further thermal annealing process. The different reasons were discussed about the origin of photoluminescence, but still, there is further need for additional studies to determine the PL mechanism.**

Keywords— O-Cat CVD, Photoluminescence, SiOC, Monomethyl Silane, Tetraethyl orthosilicate

I. INTRODUCTION

Silicon oxycarbide (SiO$_x$C$_y$) is promising material which has attracted attention due to its advantageous chemical and mechanical properties over oxide and nitride matrix (SiO$_x$ or SiN$_x$), including the compatibility in silicon-based IC's, tunable refractive index (1.45-3.10), thermal and photostability, wide bandgap and better creep resistance [1–4]. It is widely investigated for the application such as passivation layers, light-emitting applications due to its optical properties and also used as low-k dielectrics, diffusion barrier, anode material for lithium storage batteries, etc. [5–10] There are various techniques available to deposit SiO$_x$C$_y$ thin films such as hot-wire chemical vapor deposition (HWCVD) [11–14], inductively coupled plasma chemical vapor deposition (ICP-CVD) [15], plasma-enhanced chemical vapor deposition PECVD [5, 16] very high frequency (VHF) PECVD [16], thermal chemical vapor deposition (TCVD) [18-19], RF-magnetron sputtering [8] with using different precursors such as monomethyl silane (MMS), tetra-ethyl orthosilicate (TEOS), bistrimethylsilylmethane (BTMSM), tetra(trimethylsilyloxy) silane (TTMSS), tetramethylcyclotetrasiloxane (TMCTS-Si$_4$O$_4$C$_4$H$_{16}$), Silane (SiH$_4$), 2,4,6-trimethyl-2,4,6-trisila-heptane (C$_7$H$_{22}$Si$_3$), respectively [11–19].

In this work, SiO$_x$C$_y$ thin films were deposited using two different organic catalytic chemical vapor deposition (O-Cat-CVD) [20] systems, which is a modified HWCVD process using organic precursors [21]. O-Cat CVD has numerous advantages over PECVD, such as no plasma damage during the sample deposition, high deposition rate, etc. [22]. The use of safe and economic precursors is also an important advantage of O-Cat CVD. The use of alkylsilane compound precursors provides an alternative and safer source than silane because silane is a pyrophoric gas that can auto-ignite spontaneously on contact with air, and it has the lowest auto-ignition temperature in comparison to other material [23-24]. Although, O-Cat CVD system is widely used for the growth of a variety of thin films and in the previous works of our lab SiO$_x$C$_y$ thin films were obtained with this method [11–14]. However, the comparative study of the properties of SiO$_x$C$_y$ thin films has not been done by using different precursor materials with O-Cat CVD.

In this work, the effect of the variation of deposition time have studied for the as-deposited SiO$_x$C$_y$ thin films by using two different alkylsilane compound precursors, *i.e.,* Monomethyl

Silane (MMS-(CH$_3$-SiH$_3$)) and Tetra-ethyl orthosilicate [TEOS-(Si(OC$_2$H$_5$)$_4$)], respectively in two different O-Cat CVD systems. The chemical bonding structures and film compositions were investigated through Fourier transform infrared (FTIR) and X-ray Photoelectron Spectroscopy (XPS) analysis to confirm the presence of Si, O, and C elements in the deposited sample. Optical studies were carried out using photoluminescence spectroscopy, and intense emissions in a wide region of the visible spectrum were observed for the deposited thin films without further thermal annealing process.

II.   EXPERIMENT

A. Sample preparation

Thin-film samples were deposited on polished P-type crystalline silicon substrate with (100) orientation by the O-Cat CVD technique. Two different systems were used for the deposition of thin films, where the first system was used for the gaseous precursors, while the second system was used for liquid precursors. In the first O-Cat CVD system (S1), thin films were deposited by using MMS (Sigma Aldrich-462993-purity 99.9%), Oxygen (O$_2$), and Hydrogen (H$_2$) as reactant gases by using a tantalum (T$_a$) wire of 0.5 mm diameter. In contrast, TEOS (Sigma-Aldrich, reagent grade, 98%) as a liquid precursor was used and argon as a carrier gas in another system (S2) to deposit thin films by tungsten (W) wire of 0.75 mm diameter. The distance between the catalyst-wire and substrate was 5 cm in both systems, and the IR detector (Chino model IR-AHS) was used to monitor the filament temperature through the window of the corresponding chamber during the deposition period.

The deposition time was a variable parameter for the preparation of thin films in both systems. At the same time, the following conditions were used as the constant parameters for the film deposition: For both methods, the filament (T$_f$) and substrate temperature (T$_s$) were 1800ºC and 200ºC, respectively, while the flow rate of MMS, O$_2$, and H$_2$ gases were 4, 1 and 20 sccm, respectively and deposition pressure (P$_s$) of the chamber was 0.13 Torr in S1. Furthermore, 0.30 torr deposition pressure and 40 sccm Argon (Ar) flow were the constant conditions for S2.

B.   Characterization

A Gaertner ellipsometer was used to observe the refractive index and thickness of the deposited films with a variable angle from 45 to 80 degrees and a wavelength of 632.8 nm. The absorption band of different types of bonding was analyzed with the help of Fourier Transform Infrared (FTIR) spectroscopy (Nicolet 560) while the chemical analysis of SiO$_x$C$_y$ thin films was characterized by Scanning X-ray photoelectron spectroscopy (XPS) microprobe PHI 5000 VersaProbe II spectrometer using monochromatic Al X-ray source with an excitation line at 1486.6 eV. Photoluminescence (PL) emission spectrum was measured at room temperature using Kimmon Koha (Co., Ltd., Centennial, CO, USA) He-Cd laser with an excitation wavelength of 325 nm and output power of 20 mW.

III.   RESULTS AND DISCUSSION

FTIR spectra of the deposited films are shown in Fig.1, and the vibrational modes with their respective wavenumbers are also mentioned in Table I. The absorption bands of rocking, bending, and stretching modes for the Si-O-Si bonding are 470, 800, and 1080 cm^{-1}, respectively [12, 14] but the stretching mode of Si-O-Si bond for the thin films deposited with MMS in Fig. 1 (a), is observed at 1025 cm^{-1} while it appears at 1036 cm^{-1} for the films deposited with TEOS in Fig. 1 (b). Hence, deposited films with both techniques are showing the shift from the stoichiometry value of the Si-O-Si (1080 cm^{-1}) absorption band. This shift from the stoichiometry value of Si-O-Si represents the deficiency of oxygen in Si-O-Si bonding, which may generate a higher probability of having one or more silicon neighboring atoms [25-26]. This composition and/or stoichiometry changes in the oxide layer allow controlling the intensity of the luminescence and its spectral composition [27]. Moreover, an absorption band can also be observed at 1100 cm^{-1}, which represents the presence of Si-O-C bonds and confirms the formation of SiO$_x$C$_y$ thin film. Even though with the variation of deposition time from 20 min to 30 min in TEOS deposited thin films, it is also observable that the absorption band at 1100 cm^{-1} has the tendency to disappear, shifting the Si-O-Si absorption mode from 1036 to 1060 cm^{-1}, which may show this shifting behavior seems as the nature related to SiO$_x$ films.
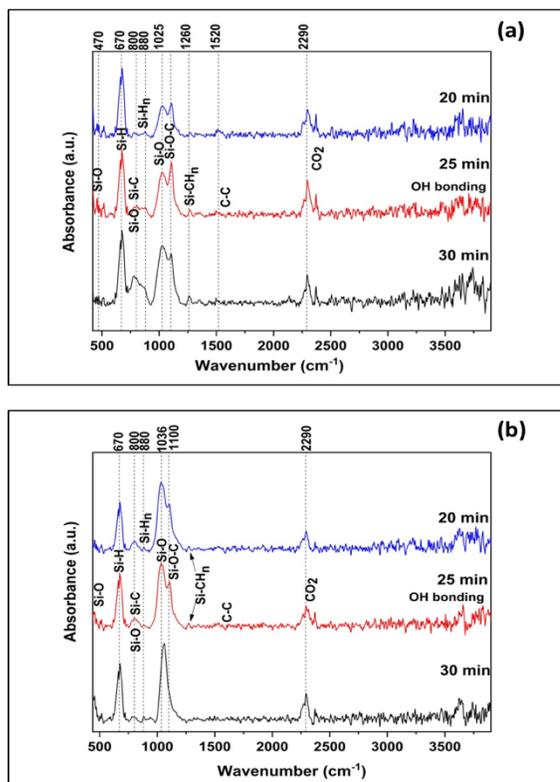
Fig. 1. FTIR spectra of the obtained films at various deposition time with a) MMS and b) TEOS material.

TABLE I.   FTIR INFRARED ABSORPTION BANDS WITH THEIR RESPECTIVE WAVENUMBERS.

Wavenumber (cm^{-1})	Vibrational mode
470	Si-O-Si rocking band
670	Si-H$_n$
800	Si-O-Si bending band, Si-C
880	Si-H$_n$
1080	Si-O-Si stretching band
1100	Si-O-C
1250	Si-H$_n$
1600	C=C
2332	CO$_2$
3100-3500	OH Bonding range

The reason of this shift in the TEOS deposited thin films can be related to the molecular structure of TEOS where four oxygen atoms are inherently bounded with Silicon atom while ethyl radicals are associated in the outer part of the molecule due to which these ethyl radicals dissociated first from the TEOS molecule [28-29]. When the deposition time increased for the TEOS deposited films, much of the carbon is transported out of the reaction zone as a by-product.

Furthermore, the absorption band at 800 cm^{-1} is also corresponding to Si–C bonds, and it can be easily observable in Fig. 1 for both materials, but here it is also noticeable that the intensity of these bonding states is proportionally increasing with the variation of time for the MMS deposited films, while it is slightly decreasing for the TEOS deposited films, respectively. The reason of the reduced intensity of the Si-C bond in TEOS deposited thin film can be the same reason as discussed previously, while the gradually increased intensity of Si-C mode can be related to the shift in the absorption band of Si-O-Si stretching mode from its stoichiometry value due to which the probability of one or more C or Si neighboring atoms become higher [25-26, 30].

In addition to these absorption bands, other bands related to Si–H$_n$, Si–H, and Si–CH$_n$ bonds were also observed at 670, 880, and 1250 cm^{-1}, respectively. The absorption band related to C=C, CO$_2$, and OH bonds are also observable at 1600, 2290, and 3600 cm^{-1}, respectively [30-32].

The chemical analysis of MMS and TEOS deposited samples for 30 min. were characterized by X-ray photoelectron spectroscopy (XPS), and it is illustrated in Fig. 2 and Fig. 3, respectively, where Si 2p, C 1s, and O 1s XPS spectrum peaks are observable. The presence of Si 2p, C 1s, and O 1s spectra confirms the existence of SiO$_x$C$_y$.

Si 2p spectra contain 5 main types of the bonding phases, which have been summarized in Table II. SiC, SiOC$_3$, SiO$_2$C$_2$, SiO$_3$C and SiO$_4$ bonding phases are observed at 99.8 101.5 eV, 102.8 eV, 103.7 eV and 104.9 eV, respectively [33].
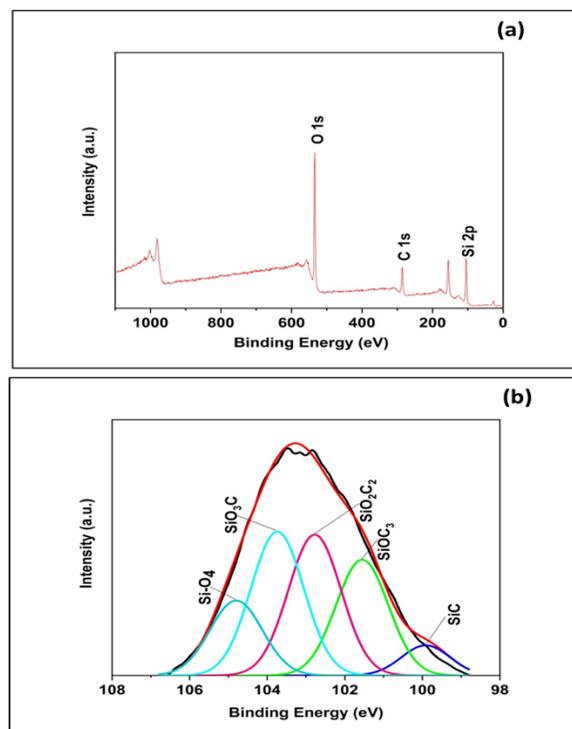
Fig. 2. a) XPS Spectrum b) Si 2p XPS for 30 min. deposited sample with MMS precursor.
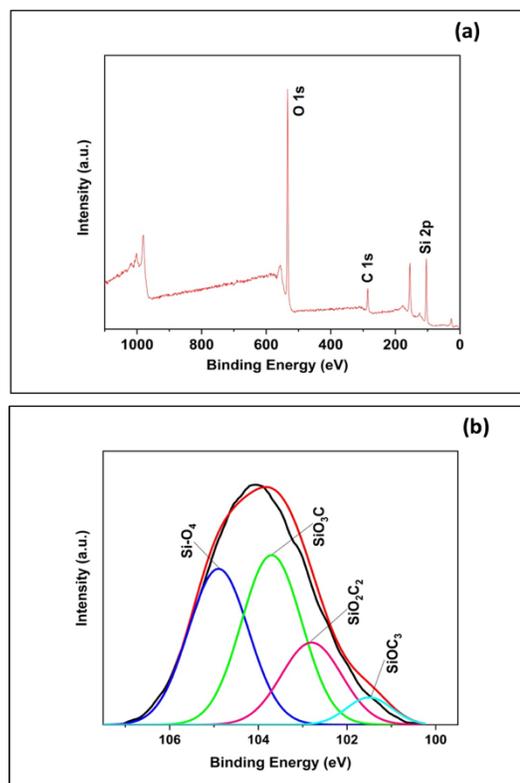
Fig. 3. a) XPS Spectrum b) Si 2p XPS for 30 min. deposited sample with TEOS precursor.

TABLE II.   THE RELATIVE CONTENT OF THE PHASES CALCULATED BY THE XPS FITTED RESULTS.

Bonding	BE (eV)	Atomic %	
		MMS	*TEOS*
SiC	99.80	5.5	-
$SiOC_3$	101.50	22.9	4.8
SiO_2C_2	102.80	28	19.2
SiO_3C	103.70	28.7	39.6
$Si-O_4$	104.90	14.8	36.4

From Table II, the high content of the SiO_4 bonding phase (36.4 %) has been observed for the deposited film with TEOS, while it is relatively low (14.8 %) for the MMS deposited films. This observation correlates with the results of FTIR, where the TEOS deposited thin films were showing its nature more related to SiO_x thin films. Furthermore, a few contents of SiC bonding phases (5.5 %) were also observed for the MMS deposited thin films while it is absent for the thin films deposited with TEOS.

The refractive index (RI) and the thickness of the deposited samples are shown in Table III. Here, the dependence of thickness and refractive index on the deposition duration is analyzed. Usually, the refractive index should be constant for every thickness in these thin films. Still, the refractive index and thickness of MMS deposited films are proportionally increasing from 1.71 to 1.77 and from 153.42 nm to 263.45 nm, respectively, with the increment of deposition time. Moreover, the thickness of TEOS deposited films is also increased proportionally with the deposition time, while the refractive index showed a random variation from 1.39 to 1.57.

Here it is observable that the refractive index of MMS deposited films is higher than TEOS deposited thin films. The reason for this difference in the refractive index can be the compositional change of thin films due to the different molecule dissociation processes TEOS and MMS, which may subsequently change the refractive index [34]. The changes in the bonding states of different thin films are easily observable from FTIR and XPS spectra, which justify the variation of time, and the composition variation of the film causes the change of refractive index.

Moreover, the temperature of the substrate may also vary due to the hitting of hot electrons in the chamber, which may change the sticking coefficient and surface mobility of radicals [35]. This might change the deposition kinetics, which can also be the reason for the variation of the refractive index.

TABLE III.   REFRACTIVE INDEX AND THICKNESS OF SAMPLES BY ELLIPSOMETRY.

Deposition Duration	MMS		TEOS	
	Thickness (nm)	*Refractive index*	*Thickness (nm)*	*Refractive index*
30 minutes	263.45	1.77	159.93	1.39
25 minutes	268.28	1.76	92.95	1.57
20 minutes	153.42	1.71	69.75	1.43

Furthermore, the refractive index of TEOS deposited thin film is close to the refractive index of SiO_2 while the refractive index of MMS deposited thin films are higher, which can be due to the aggregation of SiC bonds in the matrix of SiO_xC_y thin film.

Photoluminescence spectra are shown in fig. 4 for different deposition conditions. Broad and intense spectra are observable for the thin films deposited with both materials, *i.e.,* MMS and TEOS precursors. The variation of deposition time is proportionally affecting the intensity of PL. For MMS deposited samples, the PL peak is observed at 580 nm wavelengths or 2.13 eV for the sample deposited for 30 min while 25 min deposited film shows its PL emission at 560 nm or 2.21 eV and the PL intensity for 20 min. deposited samples is quite low, as shown in Fig. 4 (a). Moreover, TEOS deposited samples shown a peak at 477 nm wavelength or 2.65 eV, as shown in Fig. 4 (b).
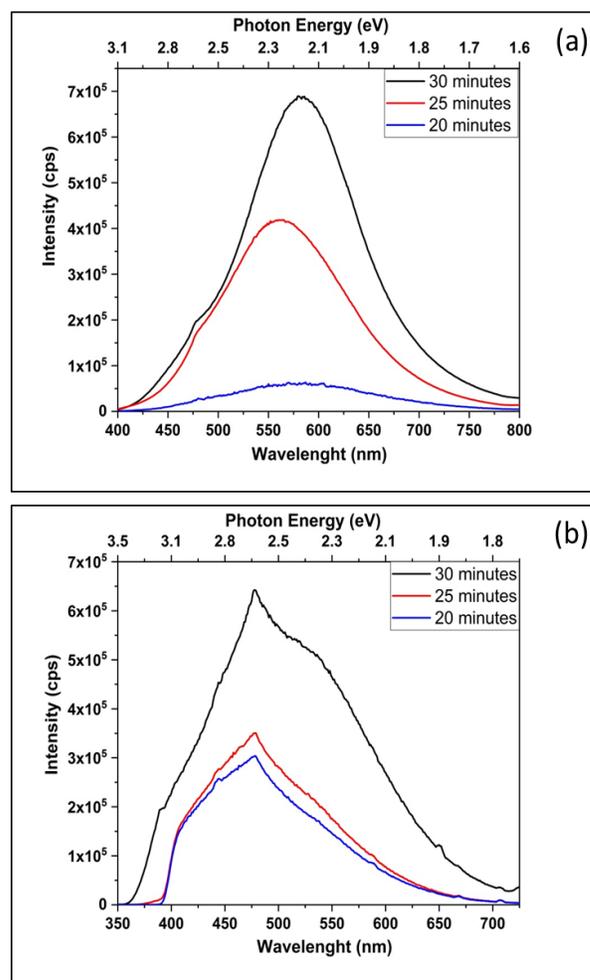
Fig. 4. PL spectra of samples obtained at different deposition duration condition with a) MMS b) TEOS material.

The origin of PL can be understood through the analysis of FTIR, where the shift in the absorption band of Si-O-Si stretching mode from its stoichiometry value represents the deficiency of oxygen in Si-O-Si bonding [25-26]. This composition and/or stoichiometry variations in the oxide layer allow controlling the intensity of the luminescence and its spectral composition [27, 36]. Hydrogen related species on the surface could be one of the responsible reasons for the origin of PL at 2.2 eV [37-38]. The intensity of the 2.2 eV band is also correlated with the concentration of the E'$_\delta$ center, which is a paramagnetic state of a silicon cluster [39].

Moreover, PL at 2.7 eV is also explained by the tunneling luminescence theory in amorphous materials, which holds one radiative and two non-radiative recombination centers [40-41].

There can be many other reasons also for the PL at 2.7 eV as a triplet–singlet transition of a molecule-like oxygen deficiency center, either the neutral oxygen vacancy; the twofold coordinated Si atom [42]; ion implantation of Si$^+$ and C$^+$ or SiC nanocluster [8, 43].

However, these defects related mechanisms may not be the only reason for the emission of the PL spectra. The Quantum confinement effect is also reported as one of the possible reasons for the origin of PL emission by some previous works [12, 13, 44].

A comprehensive study needs to understand the origin of the luminescence where the analysis of advance characterizations like PLE, TRPL, and HRTEM is further necessary to understand and explain the nature of the PL observed in the deposited SiO$_x$C$_y$ thin films.

IV.   CONCLUSIONS

The deposition of SiO$_x$C$_y$ thin films was observed by using two different alkylsilane compound precursors, *i.e.,* Monomethyl Silane (MMS) and Tetraethyl orthosilicate (TEOS). The thin films deposited with TEOS showed their nature closer to SiO$_x$ composition, which was investigated through different characterization methods as FTIR, XPS, and Ellipsometer, while the MMS deposited thin films have some similarity to SiC with the use of same deposition techniques. Moreover, the analyses of PL spectra are showing the redshift for the MMS deposited samples in comparison to TEOS deposited samples. The different reasons were discussed about the origin of photoluminescence, but still, there is further need for additional studies to determine the real PL mechanism.

REFERENCES

[1]   A. Scarmi, G. D. Sorarù, and R. Raj, "The role of carbon in unexpected visco(an)elastic behavior of amorphous silicon oxycarbide above 1273 K," J. Non. Cryst. Solids, vol. 351, pp. 2238–2243, 2005, doi: 10.1016/j.jnoncrysol.2005.06.008.

[2]   G. D. Sorarù, S. Modena, E. Guadagnino, P. Colombo, J. Egan, and C. Pantano, "Chemical Durability of Silicon Oxycarbide Glasses," J. Am. Ceram. Soc., vol. 85, no. 6, pp. 1529–36, 2002.

[3]   P. Colombo, J. R. Hellmann, and D. L. Shelleman, "Thermal Shock Behavior of Silicon Oxycarbide Foams," J. Am. Ceram. Soc., vol. 85, no. 9, pp. 2306–2312, 2002.

[4]   C. G. Pantano, A. K. Singh, and H. Zhang, "Silicon Oxycarbide Glasses," J. Sol-Gel Sci. Technol., vol. 14, pp. 7–25, 1999.

[5]   S. Kwon et al., "Single Precursor Based Ultra-Low k Thin Film Deposited with Tetrakis (trimethylsilyloxy) silane in PECVD System," Sci. Adv. Mater., vol. 10, no. 8, pp. 1147–1153, 2018, doi: 10.1166/sam.2018.3292.

[6]   V. S. Pradeep, M. Graczyk-zajac, R. Riedel, and G. D. Sorarù, "New Insights in to the Lithium Storage Mechanism in Polymer Derived SiOC Anode Materials," Electrochim. Acta, vol. 119, pp. 78–85, 2014, doi: 10.1016/j.electacta.2013.12.037.

[7]   M. Nakaya, S. Yasuhara, T. Maeda, and A. Hotta, "Impact of hot wire and material gas species on the Cat-CVD coating of gas barrier SiOC thin films onto PET bottles," Surf. Coat. Technol., vol. 344, no. February, pp. 21–29, 2018, doi: 10.1016/j.surfcoat.2018.02.101.

[8]   A. V. Vasin et al., "The effect of deposition processing on structural and luminescent properties of a-SiOC:H thin films fabricated by RF-magnetron sputtering," J. Lumin., vol. 191, pp. 102–106, 2017, doi: 10.1016/j.jlumin.2016.10.029.

[9]   S. W. King, "Dielectric Barrier , Etch Stop , and Metal Capping Materials for State of the Art and beyond Metal Interconnects," ECS J. Solid State Sci. Technol., vol. 4, no. 1, pp. N3029–N3047, 2015, doi: 10.1149/2.0051501jss.

[10]   A. Grill, S. M. Gates, T. E. Ryan, S. V Nguyen, and D. Priyadarshini, "Progress in the development and understanding of advanced low k and ultralow k dielectrics for very large-scale integrated interconnects — State of the art," Appl. Phys. Rev., vol. 011306, no. 1, pp. 1–17, 2014, doi: 10.1063/1.4861876.

[11]   A. Dutt, Y. Matsumoto, S. Godavarthi, G. Santana-Rodríguez, J. Santoyo-Salazar, and A. Escobosa, "White bright luminescence at room temperature from TEOS-based thin films via catalytic chemical vapor deposition," Mater. Lett., vol. 131, pp. 295–297, 2014, doi: 10.1016/j.matlet.2014.05.206.

[12]   J. R. Ramos-Serrano, Y. Matsumoto, and C. Morales, "Luminescent Silicon Oxycarbide Thin Films via Hot-wire CVD using Tetraethyl Orthosilicate: Role of the Chamber Pressure and Post-deposition Annealing," 2018 15th Int. Conf. Electr. Eng. Comput. Sci. Autom. Control. CCE 2018, pp. 1–4, 2018, doi: 10.1109/ICEEE.2018.8533970.

[13]   J. R. Ramos, C. Morales, and Y. Matsumoto, "Oxygen concentration effect on properties of SiOC thin films obtained by HWCVD," 2017 14th Int. Conf. Electr. Eng. Comput. Sci. Autom. Control. CCE 2017, pp. 1–4, 2017, doi: 10.1109/ICEEE.2017.8108846.

[14]   S. Godavarthi et al., "Study of porogen removal by atomic hydrogen generated by hot wire chemical vapor deposition for the fabrication of advanced low-k thin films," Thin Solid Films, vol. 575, pp. 103–106, 2015, doi: 10.1016/j.tsf.2014.10.033.

[15] T. Oh, "Comparison between SiOC Thin Films Fabricated by Using Plasma Enhance Chemical Vapor Deposition and SiO$_2$ Thin Films by Using Fourier Transform Infrared Spectroscopy," J. Korean Phys. Soc., vol. 56, no. 4, pp. 1150–1155, 2010, doi: 10.3938/jkps.56.1150.

[16] Z. Lin et al., "Defect emission and optical gain in SiC$_x$O$_y$:H films," ACS Appl. Mater. Interfaces, vol. 9, no. 27, pp. 22725–22731, 2017.

[17] V. Nikas et al., "The origin of white luminescence from silicon oxycarbide thin films," Appl. Phys. Lett., vol. 061906, no. 104, pp. 1–5, 2014, doi: 10.1063/1.4865100.

[18] A. Grill, "Plasma enhanced chemical vapor deposited SiCOH dielectrics : from low-k to extreme low-k interconnect materials," J. Appl. Phys., vol. 93, no. 3, pp. 1785–1790, 2004, doi: 10.1063/1.1534628.

[19] S. Gallis, V. Nikas, and A. Kaloyeros, "Silicon Oxycarbide Thin films and Nanostructures : Synthesis , Properties and Applications," Intech, vol. 14, no. May, pp. 277–302, 2017, doi: 10.5772/66992.

[20] H. Matsumura, "Catalytic chemical vapor deposition (CTL-CVD) method producing high quality hydrogenated amorphous silicon," Jpn. J. Appl. Phys., vol. 25, no. 12, pp. L949–L951, 1986, doi: 10.1143/JJAP.25.L949.

[21] H. Matsumura and H. Tachibana, "Amorphous silicon produced by a new thermal chemical vapor deposition method using intermediate species SiF2," Appl. Phys. Lett., vol. 47, no. 8, pp. 833–835, 1985, doi: 10.1063/1.96000.

[22] R. E. I. Schropp, "Industrialization of Hot Wire Chemical Vapor Deposition for thin film applications," Thin Solid Films, vol. 595, pp. 272–283, 2015, doi: 10.1016/j.tsf.2015.07.054.

[23] L. G. Britton, "Combustion hazards of silane and its chlorides," Plant/operations Prog., vol. 9, no. 1, pp. 16–38, 1990, doi: 10.1002/prsb.720090107.

[24] F. Tamanini, J. L. Chaffee, and R. L. Jambor, "Reactivity and Ignition Characteristics of Silane/Air Mixtures," Process Saf. Prog., vol. 17, no. 4, pp. 243–258, 1998, doi: 10.1002/prs.680170405.

[25] P. G. Pai, S. S. Chao, Y. Takagi, and G. Lucovsky, " Infrared spectroscopic study of SiO x films produced by plasma enhanced chemical vapor deposition ," J. Vac. Sci. Technol. A Vacuum, Surfaces, Film., vol. 4, no. 3, pp. 689–694, 1986, doi: 10.1116/1.573833.

[26] W. Kaiser, P. H. Keck, and C. F. Lange, "Infrared absorption and oxygen content in silicon and germanium," Phys. Rev., vol. 101, no. 4, pp. 1264–1268, 1956, doi: 10.1103/PhysRev.101.1264.

[27] A. P. Baraban, S. N. Samarin, V. A. Prokofiev, V. A. Dmitriev, A. A. Selivanov, and Y. Petrov, "Luminescence of SiO$_2$ layers on silicon at various types of excitation," J. Lumin., vol. 205, pp. 102–108, 2019, doi: 10.1016/j.jlumin.2018.09.009.

[28] G. B. Raupp, T. S. Cale, H. P. W. Hey, G. B. Raupp, and T. S. Cale, "The role of oxygen excitation and loss in plasma enhanced deposition of silicon dioxide from tetraethylorthosilicate," J. Vac. Sci. Technol. B, vol. 10, no. 1, pp. 37–45, 1992, doi: 10.1116/1.586361.

[29] S. B. Desu, "Decomposition Chemistry of Tetraethoxysilane," J. Am. Ceram. Soc., vol. 72, no. 9, pp. 1615–1621, 1989.

[30] F. Rubio, J. Rubio, and J. L. Oteo, "A FT-IR study of the hydrolysis of Tetraethylorthoselicate (TEOS)," Spectrosc. Lett., vol. 31, no. 1, pp. 199–219, 1998, doi: 10.1080/00387019808006772.

[31] S. Park, B. Parida, and K. Kim, "Thin film solar cells with Si nanocrystallites embedded in amorphous intrinsic layers by hot-wire chemical vapor deposition," J. Nanosci. Nanotechnol., vol. 13, no. 5, pp. 3397–3402, 2013, doi: 10.1166/jnn.2013.7312.

[32] H. Yamada and W. B. Person, "Absolute Infrared Intensities of the Fundamental Absorption Bands in Solid CO$_2$ and N$_2$O," J. Chem. Phys., vol. 41, no. 8, pp. 2478–2487, 1964, doi: 10.1063/1.1726291.

[33] J. Huang et al., "An interfacial crosslinking strategy to fabricate an ultrathin two-dimensional composite of silicon oxycarbide-enwrapped silicon nanoparticles for high-performance lithium storage," J. Mater. Chem. A, vol. 7, no. 40, pp. 22950–22957, 2019, doi: 10.1039/c9ta07738c.

[34] R. J. Wilby, "Determining Dielectric Constant Variation of SiOC Low k Film Using Density Measurement," no. 1, pp. 1–7.

[35] B. P. Swain and R. O. Dusane, "Effect of substrate temperature on HWCVD deposited a-SiC:H film," Mater. Lett., vol. 61, no. 25, pp. 4731–4734, 2007, doi: 10.1016/j.matlet.2007.03.029.

[36] I. Hinić, G. Stanišić, and Z. Popović, "Influence of the synthesis conditions on the photoluminescence of silica gels," J.Serb.Chem.Soc., vol. 68, no. 12, pp. 953–959, 2003.

[37] Y. D. Glinka, S. Lin, and Y. Chen, "The photoluminescence from hydrogen-related species in composites of SiO$_2$ nanoparticles," vol. 778, no. May 2013, pp. 16–19, 1999, doi: 10.1063/1.124510.

[38] Y. D. Glinka, S. Lin, and Y. Chen, "Two-photon-excited luminescence and defect formation in SiO$_2$ nanoparticles induced by 6.4-eV ArF laser light," Phys. Rev. B, vol. 62, no. 7, pp. 4733–4743, 2000.

[39] H. Nishikawa et al., "Visible photoluminescence from Si clusters in irradiated amorphous SiO2," J. Appl. Phys., vol. 3513, no. 80, pp. 3513–3517, 1996, doi: 10.1063/1.363223.

[40] S. Sato, H. Ono, S. Nozaki, and H. Morisaki, "Photoluminescence study on Oxygen-containing silicon nanostructures," Nanostructured Mater., vol. 5, no. 5, pp. 589–598, 1995, doi: 10.1016/0965-9773(95)00269-K.

[41] R. A. Street, "Luminescence in amorphous semiconductors," Adv. Phys., vol. 25, no. 4, pp. 397–453, 1976, doi: http://dx.doi.org/10.1080/00018737600101412.

[42] L. Rebohle, J. Von Borany, H. Fröb, and W. Skorupa, "Blue photo- and electroluminescence of silicon dioxide layers ion-implanted with group IV elements," Appl. Phys. B Lasers Opt., vol. 71, no. 2, pp. 131–151, 2000, doi: 10.1007/PL00006966.

[43] L. Rebohle, T. Gebel, H. Fröb, H. Reuther, and W. Skorupa, "Ion beam processing for Si/C-rich thermally grown SiO$_2$ layers: Photoluminescence and microstructure," Appl. Surf. Sci., vol. 184, pp. 156–160, 2001, doi: 10.1016/S0169-4332(01)00490-1.

[44] Y. Matsumoto et al., "Luminescence study of Si/SiC Nano-particles embedded in SiO$_x$C$_y$ matrix deposited using O-Cat-CVD," Phys. E Low-dimensional Syst. Nanostructures, vol. 111, no. March, pp. 179–184, 2019, doi: 10.1016/j.physe.2019.03.024.